processes

MDPI

Article

Investigation of Coalescence-Induced Droplet Jumping on Mixed-Wettability Superhydrophobic Surfaces

Ming-Jun Liao and Li-Qiang Duan *

National Thermal Power Engineering & Technology Research Center, Key Laboratory of Power Station Energy Transfer Conversion and System, School of Energy, Power and Mechanical Engineering, North China Electric Power University, Ministry of Education, Beijing 102206, China; liaomj666@gmail.com
* Correspondence: dlq@ncepu.edu.cn; Tel.: +86-10-61771443

Abstract: Coalescence-induced droplet jumping has received more attention recently, because of its potential applications in condensation heat transfer enhancement, anti-icing and self-cleaning, etc. In this paper, the molecular dynamics simulation method is applied to study the coalescence-induced jumping of two nanodroplets with equal size on the surfaces of periodic strip-like wettability patterns. The results show that the strip width, contact angle and relative position of the center of two droplets are all related to the jumping velocity, and the jumping velocity on the mixed-wettability superhydrophobic surfaces can exceed the one on the perfect surface with a 180° contact angle on appropriately designed surfaces. Moreover, the larger both the strip width and the difference of wettability are, the higher the jumping velocity is, and when the width of the hydrophilic strip is fixed, the jumping velocity becomes larger with the increase of the width of the hydrophobic strip, which is contrary to the trend of fixing the width of the hydrophobic strip and altering the other strip width.

Keywords: molecular dynamics simulations; mixed-wettability; superhydrophobic surfaces; jumping velocity

check for updates

Citation: Liao, M.-J.; Duan, L.-Q. Investigation of Coalescence-Induced Droplet Jumping on Mixed-Wettability Superhydrophobic Surfaces. *Processes* **2021**, *9*, 142. https://doi.org/10.3390/pr9010142

Received: 25 December 2020
Accepted: 10 January 2021
Published: 12 January 2021

Publisher's Note: MDPI stays neutral with regard to jurisdictional claims in published maps and institutional affiliations.

Copyright: © 2021 by the authors. Licensee MDPI, Basel, Switzerland. This article is an open access article distributed under the terms and conditions of the Creative Commons Attribution (CC BY) license (https://creativecommons.org/licenses/by/4.0/).

1. Introduction

In recent years, coalescence-induced droplet jumping on a superhydrophobic surface has received more and more attention [1–11], because it has been applied to various fields, including condensation heat transfer [12,13], self-cleaning [14], anti-icing [15,16], anti-dew [17] and so forth. However, the jumping velocity affects the efficiency of these applications. Obviously, promoting jumping velocity (v_j) is a beneficial approach in the applications mentioned above. Therefore, some studies have started to investigate the influence factors on v_j, and explore effective methods to make v_j higher.

Zhang et al. [18] made a comprehensive analysis of the published papers of droplet self-jumping data. They demonstrated that v_j had a definite relationship to the contact angle and droplet radius (r), where v_j followed distinct laws for different contact angle ranges and was more sensitive to a smaller radius. The number of the coalescence droplets also has an influence on v_j [3,19], which has a larger value with three and more droplets compared to two droplets' coalescence. Recently, with the development of micro–nano technology, many studies have focused on fabricating various micro-/nano-structured surfaces to discover the enhancement of droplets coalescence and jumping. In fact, it has been demonstrated that the microstructures make the apparent contact angle of the droplet increase, hence, a faster jumping of merged droplets is achieved [1,5,6,20–22]. It should be noted that this phenomenon is only suited to a droplet size larger than the microstructure size by at least one order of magnitude [23]. However, when these two sizes are comparable, what happens? It has surprisingly been found that v_j will have a dramatic improvement, even making the velocity limits for microscale droplets [7–9] with $v_j \leq 0.23u_{ic}$ and nanoscale droplets [10,11] with $v_j \leq 0.127u_{ic}$ broke. Here, u_{ic} that is equal

to $(\gamma/\rho r)^{1/2}$ represents the inertial-capillary velocity, in which γ is the surface tension and ρ is the density of liquid.

In short, there are many factors that can affect v_j, and most studies focus on the preparation of various structured surfaces. However, another surface named mixed-wettability surface which is easy to fabricate and has the potential ability to improve v_j is ignored, although some researches have proved that the condensation heat transfer performance could be adjusted with hydrophobic–hydrophilic patterned surfaces [24,25] and hybrid surfaces [26–32]. It has been found that only Xie [33] this year pointed out the unique advantages of this surface.

On the basis of the above reasons, in order to further study the influences of the surface characteristic parameters on v_j, firstly, a mixed-wettability superhydrophobic surface by alternative distribution of two different hydrophobic strips is constructed. Then, the molecular dynamics (MD) simulation method is applied to study the effects of the strip widths, contact angles and relative positions of the center of two nanodroplets on the coalescence. Finally, it is verified that the jumping velocity limit can be broken on appropriately designed surfaces.

2. Simulation Method

Figure 1 exhibits the simulated system, where the dimensions of the volume in which numerical simulation is carried out are 50 nm in x direction and 30 nm in both y and z directions. At the bottom of the box, a solid Au (100%) plate is manufactured. It is divided into two parts: one is the more hydrophobic area with yellow strips, and the other is the more hydrophilic area with gray strips. Both these two wettability areas are modeled by FCC (face-centered cubic), which is universally applied for the metal atoms. The substrate has dimensions of $50 \times 1.224 \times 30$ nm^3, containing 129,178 atoms. Two spherical argon droplets with equal radius of 8 nm are placed on the substrate, which is also modeled by FCC. The lattice constants of the substrate and droplets are 4.08 Å and 5.4 Å, respectively.

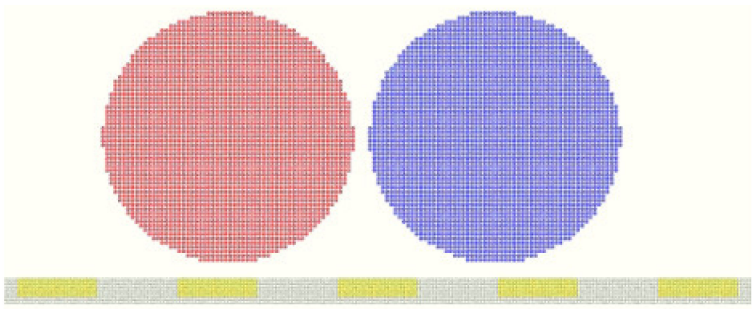


Figure 1. Initial configuration of coalescence of two argon droplets on a mixed-wettability superhydrophobic surface (the yellow region is the more hydrophobic strip, while the gray region is the more hydrophilic strip).

The potential of the embedded atom model (EAM) [34] is employed to describe the interaction between Au–Au, while the potential of Lennard–Jones 12-6 is used to simulate the interactions of Ar–Ar and Ar–Au; the function is as follows:

$$V_{ij} = 4\varepsilon\left[(\sigma/r)^{12} - c_{ij}(\sigma/r)^{6}\right] \quad (1)$$

The specific definitions of σ, ε and c_{ij} are the same as those in our previous paper [35], whose values are 3.41 Å, 10.3 meV and 1 for the Ar–Ar interaction [11], respectively. Similar to Reference [35], the interaction parameter of c_{ij} between Ar–Au is adjusted to obtain distinctive contact angles.

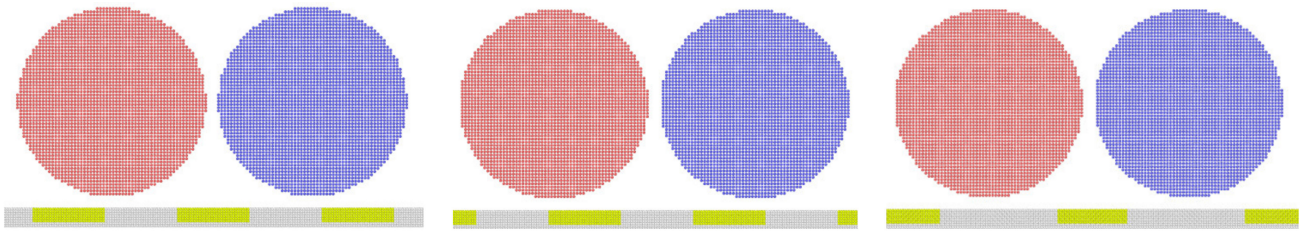
When both the initial system and interaction force field are well prepared, the equilibration process can be performed. In this process, firstly, the system is run in a canonical ensemble (NVT) for 15 ns with the temperature of 85 K by using the Nose–Hoover ther-

mostat. Subsequently, the thermostat acting on argon droplets is removed, continuing to run in a micro-canonical ensemble (NVE) for 12 ns. Finally, the system achieves an equilibrium state, where the system temperature, pressure and various potential energies are stable. Then, to reach the droplets coalescence, a horizontal velocity is given to the droplets. The droplet velocities in the range of 1 to 5 m s^{-1} are tested. The results indicate that 3 m s^{-1} is the best one for coalescence induced droplet jumping, which is consistent with the conclusion of Reference [34]. The cutoff radius in this work is set as 3σ. The Velocity–Verlet algorithm is carried out to solve the Newtonian motion equations for every atom. In all simulations, the time step is 6 fs, and atom positions and velocities are stored and calculated every 1000 time-steps.

In this paper, the contact angle θ_b of the more hydrophobic region is fixed, which is set to 180°, while θ_l of the more hydrophilic region is variable and it is set to 140°, 150° and 160°. The strip widths of these two regions are L_b and L_l, respectively. In order to study the effects of different strip widths, contact angles and with distances of the center of two moving nanodroplets on the jumping velocity, three kinds of simulations are executed. Firstly, both L_b and L_l are synchronously altered for these three different θ_l; the structures of the mixed-wettability surfaces are shown in Table 1. In this series of cases, the center of two droplets is consistent with the center of the more hydrophobic strip, which is always placed at the center of the plate (as shown Figure 2a). Secondly, under the condition that θ_l is 160°and θ_b is 180°, the two droplets are seen as a whole and the center of it is moved to the right side. The moving length is shown in Table 2. Here, the structure of the plate is as the same as the first situation, and Figure 2b shows the initial state of the distance between moving droplets is 10 nm. Lastly, if both L_b and L_l are different, and the relative contact angle is also 160°/180°, the configurations of the strip widths are shown in Table 3. In this situation, the strip width is fixed for the one, which is placed at the center of the plate, and the other is changed (as shown in Figure 2c).

Table 1. Physical dimensions of the strip width of the mixed-wettability surfaces at θ_l = 140°/150°/160° and θ_b = 180° (nm).

Case	1	2	3	4	5	6	7	8	9	10	11	12
L_b	2	3	4	5	6	8	10	12	16	18	20	24
L_l	2	3	4	5	6	8	10	12	16	18	20	24



(**a**) (**b**) (**c**)

Figure 2. The configurations of coalescence of two droplets with (**a**) $L_b = L_l$ = 6 nm; the center of two droplets is consistent with the center of more hydrophobic strip; (**b**) the two droplets paralleled moving towards the right by 6 nm on the basis of (**a**); (**c**) L_b = 6 nm, which is fixed, while L_l is changed to 10 nm, and the center of the two droplets is consistent with the fixed strip. The yellow region is the more hydrophobic strip, while the gray region is the more hydrophilic strip.

Table 2. Physical dimensions of the moving length of the center of two droplets at θ_l = 160° and θ_b = 180° (nm).

Case	1	2	3	4	5	6	7	8	9	10	11
$L_b = L_l = 5$	1	2	3	4	5	6	7	8	9	10	-
$L_b = L_l = 6$	1	2	3	4	5	6	7	8	9	10	12

Table 3. Physical dimensions of strip widths of the mixed-wettability surfaces when the strip widths are different at $\theta_l = 160^\circ$ and $\theta_b = 180^\circ$ (nm).

Case	1	2	3	4
L_b	2	3/4/5/6/8/10/12	6	7/8/9/10/12
L_l	3/4/5/6/8/10/12	2	7/8/9/10/12	6

In these three groups of simulations, 62 mixed-wettability surfaces are created, and 81 cases are used to study the effects of solid–liquid interaction degrees, initial distance between droplets and strip widths on the droplets coalescence and jumping. All simulations are performed using Large-scale Atomic/Molecular Massively Parallel Simulator (LAMMPS) [36], which is an open source code for classical MD simulation. A sample simulation file for the case of Figure 2a can be found in the Supplementary Material.

3. Results and Discussion

Figure 3a show the dimensionless jumping velocity, v_j/u_{ic}, scaled with the inertial-capillary velocity. On the flat surfaces with the contact angle of 180°, the maximum dimensionless jumping velocity was reported as 0.127 [10,11]. However, the result of this paper shows that the velocity limit is broken on the mixed-wettability superhydrophobic surfaces with equal width of L_b and L_l. For this design, v_j/u_{ic} exceeds the limit only at larger strip width, and the maximum ($v_j/u_{ic} = 0.21$) occurs when θ_l is 140° and both L_b and L_l are 10 nm. When the center of two droplets is moved, v_j/u_{ic} is shown in Figure 3b. For the larger move length (8 nm), v_j/u_{ic} will exceed the limit; thus, there is a best position for the maximum velocity. For the cases when L_b and L_l are different, v_j/u_{ic} is shown in Figure 3c,d. As L_l is increasing, regardless of whether L_b is large or small, v_j/u_{ic} is generally less than the velocity when $L_b = L_l$. On the contrary, when L_l is fixed, v_j/u_{ic} can always exceed the limit with the increase of L_b.

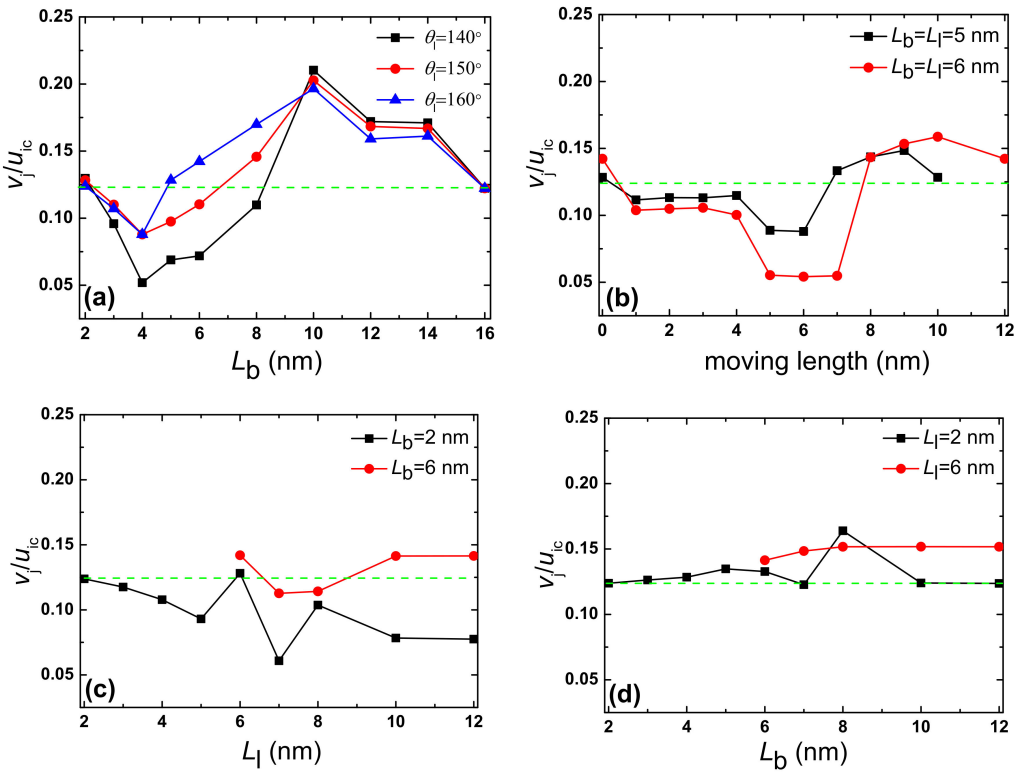


Figure 3. Dependency of the dimensionless jumping velocity of the coalesced droplets with respect to the effect of (**a**) strip widths and contact angles when $L_b = L_l$; (**b**) moving length of the center of two droplets when $L_b = L_l$; (**c**) hydrophilic strip width when the hydrophobic strip width is fixed; (**d**) the hydrophobic strip width when the hydrophilic strip width is fixed; where the dashed line denotes the limit value 0.127.

3.1. Mixed-Wettability Superhydrophobic Surfaces with Equal Strip Width

For the design of mixed-wettability superhydrophobic surfaces with equal widths of a hydrophobic strip and a more hydrophilic strip, the jumping velocity is raised only for a larger strip width, and both the minimum and maximum velocities appear when both L_b and L_l are 4 nm or 10 nm in these three contact angle situations (as shown in Figure 3a). The reason for this trend is that the narrow strip has little influence on the apparent contact angle (as shown in Figure 4a), so it is nearly the same as a uniform surface with the contact angle of 180°. However, the energy dissipation caused by adhesion is larger than that surface, which makes the velocity decrease at the smaller strip width ($L_b = L_l \leq 4$ nm). With the strip width continuing to increase ($L_b = L_l \leq 10$ nm), the apparent contact angle is decreased (as shown in Figure 4b), making the height of the mass center of the droplets smaller. Figure 4c–f extract the heights of the mass center to exhibit the relations between contact angles and strip widths, which shows that the larger the strip width is, the smaller the height of mass center is. Moreover, the larger strip width makes the liquid bridge impact the solid plate with a larger velocity, just as shown in Figure 4g. Subsequently, the larger impacting velocity generates more intensively upward counterforce, which makes the coalesced droplet shrink and jump in a faster speed. Therefore, the curves from Figure 4c–f reveal that the merged droplets can deviate from surfaces more easily with $L_b = L_l = 10$ nm than other strip widths, and the situation of $L_b = L_l = 4$ nm has the most gentle trend. It is also found that both the contact angle and height of mass center have an inversely proportional relationship when both L_b and L_l are 10 nm in three different θ_l just as shown in Figure 4g, which reveals that the maximum velocity appears when θ_l is 140° and the minimum velocity appears when θ_l is 160°. If the strip width continues to increase, the velocity will slightly decrease (10 nm $\leq L_b = L_l \leq 12$ nm) and then remains stable ($L_b = L_l \geq 12$ nm). The stage of decreasing is caused by the coaction of energy dissipation of adhesion and the height of the mass center. It is clear that the larger the strip width is, the greater the adhesive work is; however, the height of the mass center has little variation from Figure 4c–f, which means the counterforces are nearly identical in the situations of $L_b = L_l = 10$ nm and $L_b = L_l = 12$ nm. Therefore, the jumping velocity will decrease due to the greater energy dissipation. The reason for the stable stage is that for a wider strip ($L_b = L_l \geq 12$ nm), the more hydrophilic contact areas of the liquid bridges just impacting the substrate are almost the same (as shown in Figure 4h,i); thus, the energy dissipation caused by adhesion is approximately equal, the same as the height of the mass center of the coalesced droplet. Both of these two factors make the velocity stable.

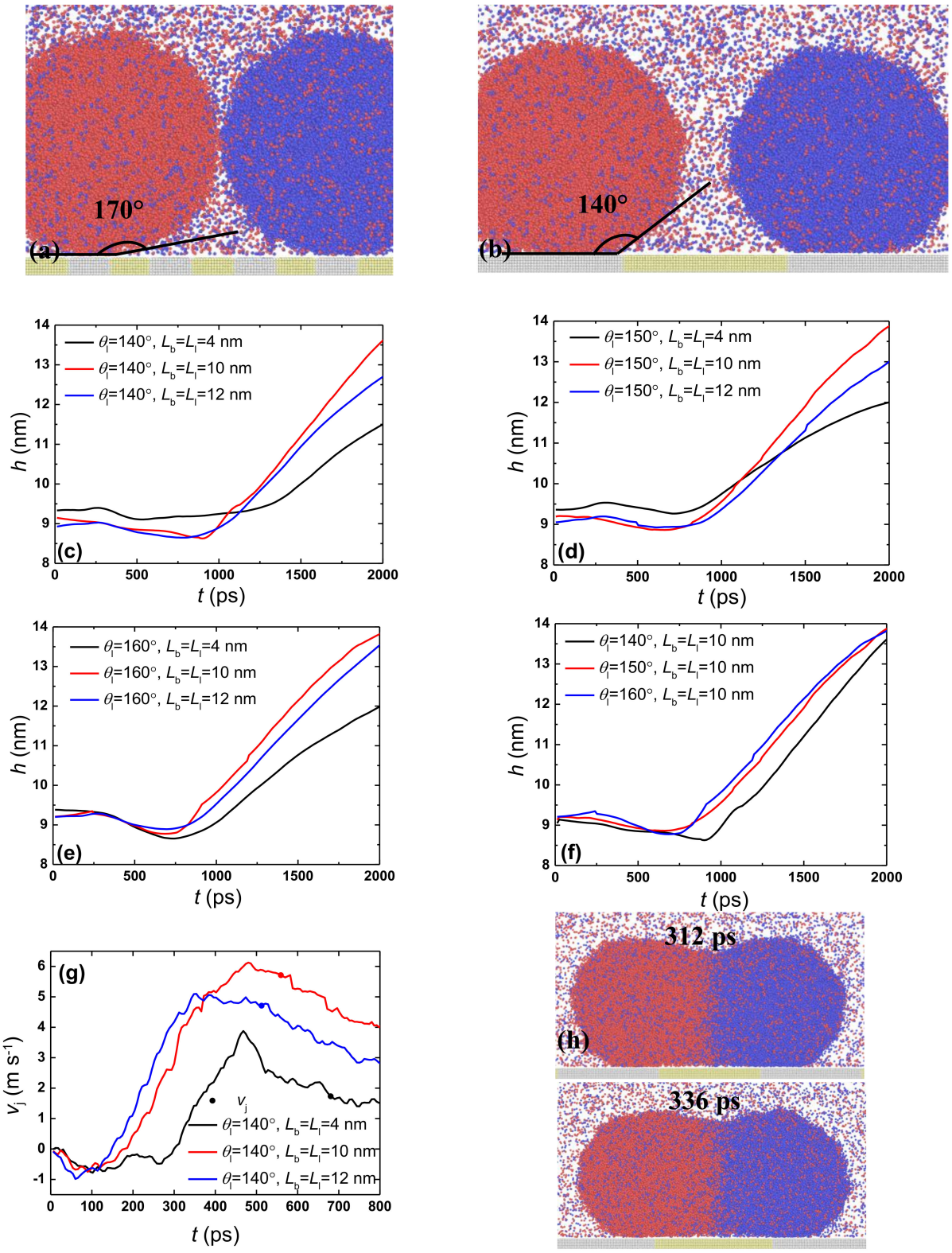


Figure 4. (**a**,**b**) Contact angles for $L_b = L_l = 2$ nm and $L_b = L_l = 10$ nm. (**c**–**f**) Evolution of droplets height of the mass center on different surfaces. (**g**) Transient component velocity in y-direction perpendicular to the surface and the value of jumping velocity in three different strip widths at contact angle of 140°. (**h**,**i**) The states of liquid bridge just impacting the substrate when $L_b = L_l = 12$ nm and $L_b = L_l = 14$ nm.

3.2. Mixed-Wettability Superhydrophobic Surfaces with Center Moved

For the cases of the center of the two droplets being moved to the right side, typical time-lapse snapshots of coalescence process are illustrated in Figure 5a–c, where the coalescence-induced droplet jumping takes place more difficultly with the center of two droplets moving by 5 nm, and more easily with the center moving by 10 nm. This can be explained from two aspects: on the one hand, the snapshots show when the center moves, the liquid bridge impacts the surfaces with different wettability, and this will certainly affect the coalescence and jumping process; on the other hand, from the evolution of the droplets height of the mass center, which is plotted in Figure 5d, the height of the mass center before the coalescence has some differences, and absolutely it will affect the upward counterforce. Both kinds of factors make the jumping velocity exhibit the trend in Figure 3b. When the impact area is more hydrophobic, it is more feasible for the progress of coalescence, and when the height of the mass center is lower, the distance for liquid bridge impacting on the surface is shorter and the impaction becomes stronger. These two reasons make the jumping velocity larger, and the situation of moving length with 10 nm holds these two factors indeed.

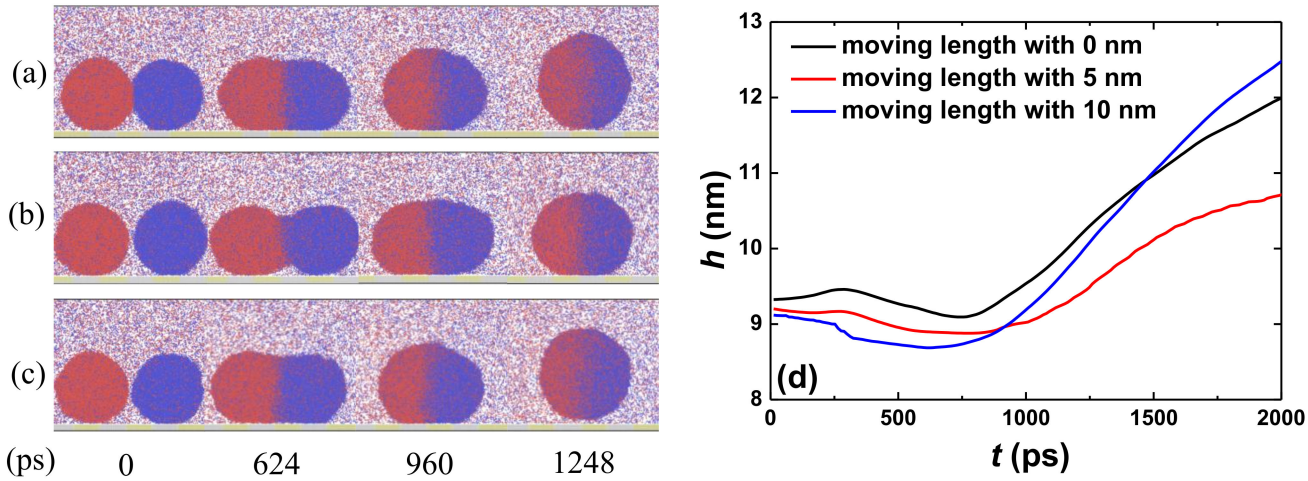


Figure 5. Snapshots of the coalesced droplets at $L_b = L_l = 6$ nm, $\theta_l = 160°$: (**a**) the center is unmoved; (**b**) the center is moved by 5 nm; (**c**) the center is moved by 10 nm; (**d**) evolution of the droplets height of mass center with different moving distance.

3.3. Mixed-Wettability Superhydrophobic Surfaces with Unequal Strip Width

For mixed-wettability surfaces with unequal strip widths, so long as the width of the more hydrophobic strip is fixed, increasing the width of the other strip will make more adhesive dissipation; nevertheless, if the width of the more hydrophilic strip is fixed, adjusting the width of the other strip can decrease the dissipation. Therefore, the trends of the jumping velocity in these two situations can be explained by the energy theory. This phenomenon can also be analyzed another way: when the expanding liquid bridge impacts the substrate, the high pressure on the surface will be built up undoubtedly. The high pressure accelerates the coalescence process, which results in the coalesced droplets bouncing from substrate quickly. The stage of the pressure exceeding the average value actually corresponds to the moment of the component velocity v_y exactly increasing from its minimum to its maximum, which was also discussed in Reference [10]. The average pressure on the surfaces with different strip width as a function of time are illustrated in Figure 6, where these three configurations have nearly equal average pressure, but a higher peak pressure obviously occurs for the surface with $L_b = 6$ nm, $L_l = 2$ nm, indicating a stronger bridge impact and leading to a higher peak of v_y.

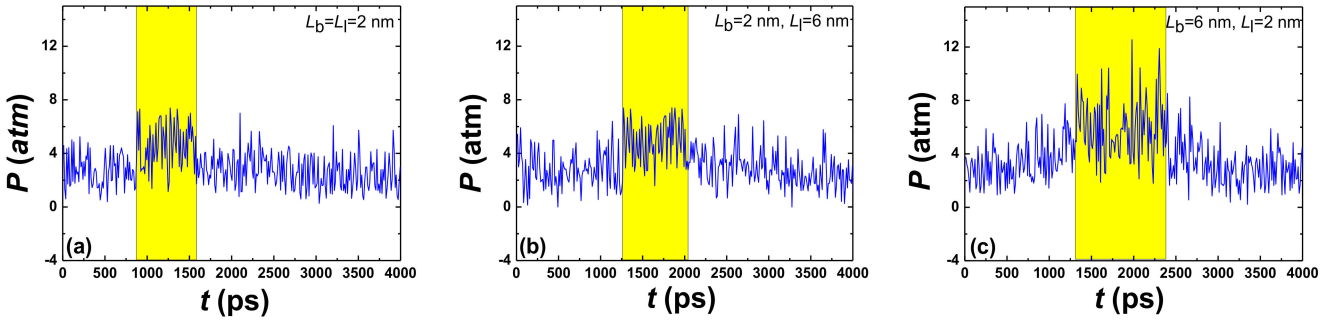


Figure 6. The average pressure on the surfaces at $\theta_l = 160^\circ$ with (**a**) $L_b = L_l = 2$ nm, (**b**) $L_b = 2$ nm, $L_l = 6$ nm and (**c**) $L_b = 6$ nm, $L_l = 2$ nm. The left ordinate of the yellow region denotes the time when the pressure starts to increase, while the right one denotes the time the pressure returns to the previous value.

4. Conclusions

In this paper, coalescence-induced droplet jumping on mixed-wettability superhydrophobic surfaces is studied numerically by using the molecular dynamics simulation method. The effects of the strip widths, contact angles and the relative positions of the center of two droplets on the jumping velocity are deeply investigated. It is found that the jumping velocity on mixed-wettability superhydrophobic surfaces can exceed the one on a perfect surface with the contact angle of 180°. It is also discovered that the larger the strip width is, the higher the jumping velocity is, and the less the wettability differences between two strips is, the lower the jumping velocity is, and when the width of more hydrophilic strip is fixed, the jumping velocity will increase with the width of the other strip increasing, which is contrary to the trend of fixing the width of the more hydrophilic strip and altering the other strip width.

Supplementary Materials: The following are available online at https://www.mdpi.com/2227-9717/9/1/142/s1. Case 1: Supplementary Equilibrium Codes and Supplementary Running Codes.

Author Contributions: M.-J.L. wrote the manuscript. L.-Q.D. supervised and supported this study and critically revised the manuscript. All authors have read and agreed to the published version of the manuscript.

Funding: This research was funded by the National Nature Science Foundation Projects of China, (No. 52076078 and No. 52090064) and the Science Fund for Creative Research Groups of the National Natural Science Foundation of China, (No. 51821004).

Institutional Review Board Statement: Not applicable.

Informed Consent Statement: Not applicable.

Data Availability Statement: Data sharing not applicable.

Conflicts of Interest: The authors declare no conflict of interest.

References

1. Boreyko, J.B.; Chen, C.H. Self-Propelled Dropwise Condensate on Superhydrophobic Surfaces. *Phys. Rev. Lett.* **2009**, *103*, 184501. [CrossRef] [PubMed]
2. Nam, Y.; Kim, H.; Shin, S. Energy and Hydrodynamic Analyses Of Coalescence-Induced Jumping Droplets. *Appl. Phys. Lett.* **2013**, *103*, 161601. [CrossRef]
3. Wang, K.; Liang, Q.; Jiang, R.; Zheng, Y.; Lan, Z.; Ma, X. Numerical Simulation of Coalescence-Induced Jumping of Multidroplets on Superhydrophobic Surfaces: Initial Droplet Arrangement Effect. *Langmuir* **2017**, *33*, 6258–6268. [CrossRef] [PubMed]
4. Qu, X.; Boreyko, J.B.; Liu, F.; Agapov, R.L.; Lavrik, N.V.; Retterer, S.T.; Chen, C.H. Self-Propelled Sweeping Removal of Dropwise Condensate. *Appl. Phys. Lett.* **2015**, *106*, 221601. [CrossRef]
5. Enright, R.; Miljkovic, N.; Al-Obeidi, A.; Thompson, C.V.; Wang, E.N. Condensation on Superhydrophobic Surfaces: The Role of Local Energy Barriers and Structure Length Scale. *Langmuir* **2012**, *28*, 14424–14432. [CrossRef]

6. Zhang, K.; Liu, F.; Williams, A.J.; Qu, X.; Feng, J.J.; Chen, C.-H. Self-Propelled Droplet Removal from Hydrophobic Fiber-Based Coalescers. *Phys. Rev. Lett.* **2015**, *115*, 074502. [CrossRef]
7. Liu, F.; Ghigliotti, G.; Feng, J.J.; Chen, C.H. Numerical simulations of self-propelled jumping upon drop coalescence on non-wetting surfaces. *J. Fluid Mech.* **2014**, *752*, 39–65. [CrossRef]
8. Enright, R.; Miljkovic, N.; Sprittles, J.; Nolan, K.; Mitchell, R.; Wang, E.N. How Coalescing Droplets Jump. *ACS Nano* **2014**, *8*, 10352–10362. [CrossRef]
9. Wang, F.C.; Yang, F.; Zhao, Y.P. Size Effect on The Coalescence-Induced Self-Propelled Droplet. *Appl. Phys. Lett.* **2011**, *98*, 053112. [CrossRef]
10. Liang, Z.; Keblinski, P. Coalescence-Induced Jumping of Nanoscale Droplets on Super-Hydrophobic Surfaces. *Appl. Phys. Lett.* **2015**, *107*, 143105. [CrossRef]
11. Xie, F.F.; Lu, G.; Wang, X.D.; Wang, B.B. Coalescence-Induced Jumping of Two Unequal-Sized Nanodroplets. *Langmuir* **2018**, *34*, 2734–2740. [CrossRef] [PubMed]
12. Miljkovic, N.; Enright, R.; Nam, Y.; Lopez, K.; Dou, N.; Sack, J.; Wang, E.N. Jumping-Droplet-Enhanced Condensation on Scalable Superhydrophobic Nanostructured Surfaces. *Nano Lett.* **2013**, *13*, 179–187. [CrossRef] [PubMed]
13. Rykaczewski, K.; Paxson, A.T.; Anand, S.; Chen, X.; Wang, Z.; Varanasi, K.K. Multimode Multidrop Serial Coalescence Effects during Condensation on Hierarchical Superhydrophobic Surfaces. *Langmuir* **2013**, *29*, 881–891. [CrossRef] [PubMed]
14. Wisdom, K.M.; Watson, J.A.; Qu, X.; Liu, F.; Watson, G.S.; Chen, C.H. Self-Cleaning of Superhydrophobic Surfaces by Self-Propelled Jumping Condensate. *Proc. Natl. Acad. Sci. USA* **2013**, *110*, 7992–7997. [CrossRef]
15. Zhang, Q.; He, M.; Chen, J.; Wang, J.; Song, Y.; Jiang, L. Anti-Icing Surfaces Based on Enhanced Self-Propelled Jumping of Condensed Water Microdroplets. *Chem. Commun.* **2013**, *49*, 4516–4518. [CrossRef]
16. Chen, X.; Ma, R.; Zhou, H.; Zhou, X.; Che, L.; Yao, S.; Wang, Z. Activating the Microscale Edge Effect in a Hierarchical Surface for Frosting Suppression and Defrosting Promotion. *Sci. Rep.* **2013**, *3*, 2515. [CrossRef]
17. Feng, J.; Pang, Y.; Qin, Z.; Ma, R.; Yao, S. Why Condensate Drops Can Spontaneously Move Away on Some Superhydrophobic Surfaces but Not on Others. *ACS Appl. Mater. Interfaces* **2012**, *4*, 6618–6625. [CrossRef]
18. Li, H.; Yang, W.; Aili, A.; Zhang, T. Insights into The Impact of Surface Hydrophobicity On Droplet Coalescence And Jumping Dynamics. *Langmuir* **2017**, *33*, 8574–8581. [CrossRef]
19. Chu, F.; Yuan, Z.; Zhang, X.; Wu, X. Energy Analysis of Droplet Jumping Induced By Multi-Droplet Coalescence: The Influences Of Droplet Number And Droplet Location. *Int. J. Heat Mass Trans.* **2018**, *121*, 315–320. [CrossRef]
20. Mulroe, M.D.; Srijanto, B.R.; Ahmadi, S.F.; Collier, C.P.; Boreyko, J.B. Tuning Superhydrophobic Nanostructures to Enhance Jumping-Droplet Condensation. *ACS Nano* **2017**, *11*, 8499–8510. [CrossRef]
21. Kim, A.; Lee, C.; Kim, H.; Kim, J. Simple Approach to Superhydrophobic Nanostructured Al for Practical Antifrosting Application Based on Enhanced Self-propelled Jumping Droplets. *ACS Appl. Mater. Interface* **2015**, *7*, 7206–7213. [CrossRef] [PubMed]
22. Vahabi, H.; Wang, W.; Davies, S.; Mabry, J.M.; Kota, A.K. Coalescence-Induced Self-Propulsion of Droplets on Superomniphobic Surfaces. *ACS Appl. Mater. Interfaces* **2017**, *9*, 29328–29336. [CrossRef] [PubMed]
23. Lu, G.; Wang, X.D.; Duan, Y.Y. A Critical Review of Dynamic Wetting by Complex Fluids: From Newtonian Fluids to Non-Newtonian Fluids and Nanofluids. *Adv. Colloid Interface Sci.* **2016**, *236*, 43–62. [CrossRef] [PubMed]
24. Derby, M.M.; Chatterjee, A.; Peles, Y.; Jensen, M.K. Flow Condensation Heat Transfer Enhancement in A Mini-Channel with Hydrophobic and Hydrophilic Patterns. *Int. J. Heat Mass Transf.* **2014**, *68*, 151–160. [CrossRef]
25. Chatterjee, A.; Derby, M.M.; Peles, Y.; Jensen, M.K. Enhancement of Condensation Heat Transfer with Patterned Surfaces. *Int. J. Heat Mass Transf.* **2014**, *71*, 675–681. [CrossRef]
26. Ma, X.H.; Wang, B.B.; Xu, D.Q.; Lin, J.F. Filmwise Condensation Heat Transfer Enhancement with Dropwise and Filmwise Coexisting Condensation Surfaces. *Chin. J. Chem. Eng.* **1998**, *6*, 5–12.
27. Ma, X.H.; Song, T.Y.; Lan, Z.; Zhou, X.D. Experimental Investigation of Enhancement of Dropwise Condensation Heat Transfer of Steam-Air Mixture: Falling Droplet Effect. *J. Enhanc. Heat Transf.* **2007**, *7*, 295–305. [CrossRef]
28. Grooten, M.H.M.; van der Geld, C.W.M. Surface property effects on dropwise condensation heat transfer from flowing air-steam mixtures to promote drainage. *Int. J. Therm. Sci.* **2012**, *54*, 220–229. [CrossRef]
29. Kumagai, S.; Tanaka, S.; Katsuda, H.; Shimada, R. On the Enhancement of Filmwise Condensation Heat Transfer by Means of the Coexistence with Dropwise Condensation Sections. *Exp. Heat Transf.* **1991**, *4*, 71–82. [CrossRef]
30. Varanasi, K.K.; Hsu, M.; Bhate, N.; Yang, W.; Deng, T. Spatial Control in The Heterogeneous Nucleation of Water. *Appl. Phys.* **2009**, *95*, 094101. [CrossRef]
31. Yamauchi, A.; Kumagai, S.; Takeyama, T. Condensation Heat Transfer on Various Dropwise- Filmwise Coexisting Surface. *Trans. Jpn. Soc. Mech. Eng. Ser. B* **1985**, *51*, 2606–2613. [CrossRef]
32. Ma, X.H. Condensation Heat Transfer of Steam on Vertical Dropwise and Filmwise Coexisting Surfaces with a Thick Organic Film Promoting Dropwise Mode. *Exp. Heat Transf.* **2003**, *16*, 239–253. [CrossRef]
33. Xie, F.F.; Wang, D.Q.; Wang, Y.B.; Yang, Y.R.; Wang, X.D. Coalescence-Induced Jumping of Nanodroplets on Mixed-Wettability Superhydrophobic Surfaces. *Can. J. Phys.* **2020**, in press. [CrossRef]
34. Foiles, S.M.; Baskes, M.I.; Daw, M.S. Embedded-atom-method Functions for the Fcc Metals Cu, Ag, Au, Ni, Pd, Pt, and Their Alloys. *Phys. Rev. B* **1986**, *33*, 7983. [CrossRef] [PubMed]

35. Liao, M.J.; Duan, L.Q. Explosive Boiling Of Liquid Argon Films on Flat and Nanostructured Surfaces. *Numer. Heat Tr. A Appl.* **2020**, *78*, 94–105. [CrossRef]
36. Plimpton, S. Fast Parallel Algorithms for Short-Range Molecular Dynamics. *J. Comput. Phys.* **1995**, *117*, 1–19. [CrossRef]